ISSN (Print) 1226-1750
ISSN (Online) 2233-6656
**Journal of Magnetics** 23(4), 541-545 (2018) https://doi.org/10.4283/JMAG.2018.23.4.541

# Effect of Y addition on Glass Forming Ability and Magnetic Properties in Fe-based Amorphous Ribbons

**Jihye Kim, Sumin Kim, and Haein-Choi Yim***

*Department of Physics, Sookmyung Women's University, Seoul 04310, Republic of Korea*

(Received 4 October 2018, Received in final form 1 November 2018, Accepted 5 November 2018)

**In the present study, the effect of Y addition on the glass forming ability and magnetic properties of $[Fe_{0.75}B_{0.20}Si_{0.05}]_{100-x}Y_x$ (x = 0, 1, 2, 3, 4) amorphous ribbons were investigated. The ribbons of 2 mm in width and 30 μm in thickness were obtained using the melt spinning technique. All ribbons were identified as fully amorphous by using X-ray diffraction. The thermal properties, including glass transition temperature, crystallization temperature, and supercooled liquid region, were measured by differential scanning calorimetry and thermomechanical analysis. The results showed that, with an increase of the Y content, the supercooled liquid region broadened, indicating an improvement of glass forming ability. The magnetic properties of the amorphous ribbons were measured by a vibrating sample magnetometer. In addition, it was confirmed that, with an increase of the Y content, coercivity tended to decrease.**

**Keywords :** Fe-based, amorphous, glass forming ability, Y addition

## 1. Introduction

Soft magnetic materials play an increasingly important role in industry for instance, in the production of distribution transformers, sensors, electromagnetic shielding applications, actuators, as well as data storage devices [1-4]. For several decades, numerous studies on amorphous alloys as soft magnetic materials have been actively carried out [5-7]. In particular, due to the excellent soft magnetic properties, such as high saturation magnetization ($M_s$) and low coercivity ($H_c$) [8-12], Fe-based amorphous alloys have attracted much attention in a variety of emerging science fields and engineering. Among the Fe-based amorphous alloys developed over decades, the Fe-Si-B amorphous alloys have been widely used due to their excellent soft magnetic properties [13]. However, Fe-based amorphous alloys have dimensional limitations due to the limited glass forming ability (GFA) of amorphous alloys [14, 15]. In order to improve the GFA in Fe-based amorphous alloys, Fe are usually replaced with various glass forming metallic elements, such as Cu, Nb, Zr, Mo, and Ta concentration [12, 16, 17]. According to the empirical rules [18], a large difference of the atomic radius between Y and Fe leads to improvement the GFA, and also it causes an increase the atomic packing density of the amorphous structure, so the atomic diffusion more difficult [19, 20]. Y has a large atomic radius of 212 pm, which is much larger than that of Fe (156 pm), Si (111 pm), B (87 pm), Ta (200 pm), Cr (166 pm), Mo (190 pm), and Nb (198 pm). Therefore, Y is the best candidate for improving GFA. Moreover, the large negative heat of mixing value between Y and B (−35 kJ/mol), as compared to that between Fe and B (−11 kJ/mol), causes a change of the local atomic structure in the liquid phase [21]. These effects prompt the formation of the network of a short-range ordered atomic configuration which is necessary for the progress of crystallization, leading to the stabilization of supercooled liquid [22].

In the present study, we aimed to investigate the effect of Y addition on GFA and magnetic properties of the $[Fe_{0.75}B_{0.20}Si_{0.05}]_{100-x}Y_x$ system. Furthermore, for comparison, we also conducted the experiment of the Y-free alloys (x = 0).

## 2. Experiments

Multi-component ingots with $[Fe_{0.75}B_{0.20}Si_{0.05}]_{100-x}Y_x$ (x = 0, 1, 2, 3, 4) were prepared by arc-melting under the Ti-gettered argon atmosphere. The alloys were prepared


*Corresponding author: Tel: +82-2-710-9239
Fax: +82-303-0799-0362, e-mail: haein@sookmyung.ac.kr

using high-purity metals of Fe (99.95 %), B (99.5 %), Si (99.999 %), and Y (99.9 %). In order to maximize compositional homogeneity, each ingot was re-melted at least four times. The amorphous ribbons were rapidly solidified by the melt-spinning method with the wheel speed of 39.3 m/s under the argon atmosphere. The melt-spun ribbons were typically 2 mm in width and 30 μm in thickness. The structures of amorphous alloys were confirmed by X-ray diffraction (XRD) with Cu-Kα radiation. The primary crystallization temperature ($T_{x,DSC}$) was investigated by differential scanning calorimetry (DSC) under the argon atmosphere with the heating rate of 0.34 K/s. Due to the brittle nature of the Y additions ribbons (x = 1, 2, 3, 4), the glass transition temperature ($T_g$) and crystallization temperature ($T_{x,TMA}$) were measured using the thermomechanical analysis (TMA) in the compressive mode. This measurement was conducted with the heating rate 0.34 K/s, force of 3 N, and the initial height of 0.3 mm. The values of $M_s$ and $H_c$ were measured by a vibrating sample magnetometer (VSM) under the maximum applied field of 10,000 Oe and a DC B-H curve tracer under the maximum applied field of 300 Oe, respectively.

## 3. Results and Discussion

Figure 1 shows the XRD patterns of as-quenched ribbons with different Y addition. Based on the results, it consists only of a broad halo humps without any crystalline peak, suggesting that all the ribbons are fully amorphous independent of Y additions.

Figure 2 shows the DSC curves of the melt-spun $[Fe_{0.75}B_{0.20}Si_{0.05}]_{100-x}Y_x$ (x = 0, 1, 2, 3, 4) amorphous ribbons. The DSC curves indicate the exothermic peak due to the crystallization. Except for the $Fe_{74.25}B_{19.8}Si_{4.95}Y_1$ (x = 1) alloy, only one exothermic peak with a high intensity is observed for each ribbons, which suggests the involvement of a single-stage crystallization process. However, the alloy with x = 1 has a two-stage crystallization process. $T_{x,DSC}$ values obtained in the DSC experiment are marked with the arrows in Fig. 2, and the values are listed in Table 1. With an increase in the Y content from 0 to 4 at.%, $T_{x,DSC}$ values increased from 818 to 910 K. The crystallization reaction shifted to higher temperature, as the phase change kinetics slowed down.

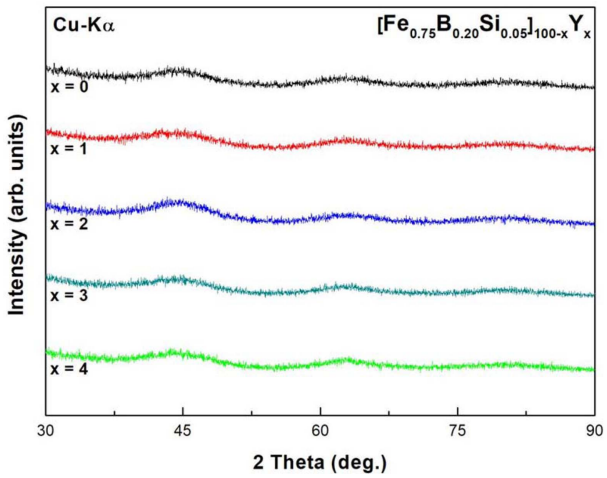


**Fig. 1.** (Color online) X-ray diffraction patterns of the $[Fe_{0.75}B_{0.20}Si_{0.05}]_{100-x}Y_x$ (x = 0, 1, 2, 3, 4) melt-spun ribbons.

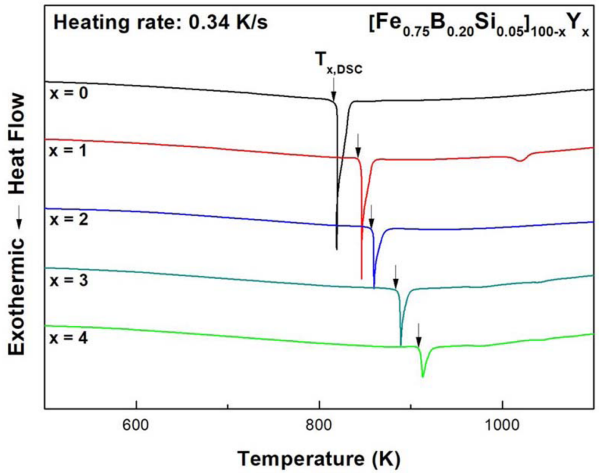


**Fig. 2.** (Color online) DSC curves of the $[Fe_{0.75}B_{0.20}Si_{0.05}]_{100-x}Y_x$ (x = 0, 1, 2, 3, 4) melt-spun amorphous ribbons.

Thereafter, since no glass transition phenomenon through the DSC experiment was observed for Fe-rich amorphous alloys [23], the Fe-Si-B-Y amorphous alloys were investi-

**Table 1.** Thermal properties of the $[Fe_{0.75}B_{0.20}Si_{0.05}]_{100-x}Y_x$ (x = 0, 1, 2, 3, 4) melt-spun amorphous ribbons.

| x | Alloys | | | | Thermal Properties (K) | | | | |
|---|---|---|---|---|---|---|---|---|---|
| | | | | | $T_g$ | $T_{x,TMA}$ | $T_{x,DSC}$ | $\Delta T_x$ (= $T_{x,TMA} - T_g$) | $T_{vs}$ |
| 0 | $Fe_{75}$ | $B_{20}$ | $Si_5$ | | 801 | 819 | 818 | 18 | 818 |
| 1 | $Fe_{74.25}$ | $B_{19.8}$ | $Si_{4.95}$ | $Y_1$ | 826 | 845 | 844 | 19 | 844 |
| 2 | $Fe_{73.5}$ | $B_{19.6}$ | $Si_{4.9}$ | $Y_2$ | 841 | 861 | 860 | 20 | 860 |
| 3 | $Fe_{72.75}$ | $B_{19.4}$ | $Si_{4.85}$ | $Y_3$ | 858 | 888 | 887 | 30 | 877 |
| 4 | $Fe_{72}$ | $B_{19.2}$ | $Si_{4.8}$ | $Y_4$ | 870 | 911 | 910 | 41 | 889 |

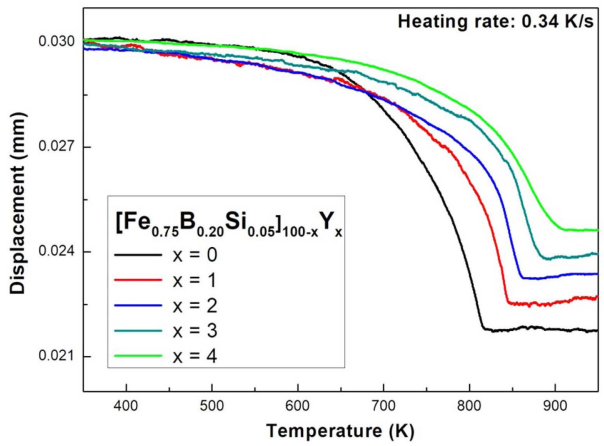


**Fig. 3.** (Color online) Temperature dependence of the displacement for the $[Fe_{0.75}B_{0.20}Si_{0.05}]_{100-x}Y_x$ (x = 0, 1, 2, 3, 4) melt-spun amorphous ribbons.

gated by TMA to measure the $T_g$. The results of the TMA experiment are presented as a dimensional change versus temperature plot, which are shown in Fig. 3. As can be seen in Fig. 3, with an increase of the Y content, displacement length decreased, which is related to viscous flow. $T_{x,TMA}$ is determined as the point at which thermal expansion occurs according to crystallization on the plot [24]. In fact, a stronger thermal expansion already existed in the glass transition region (below $T_{x,TMA}$) [25], but it was obscured by structure relaxation. $T_g$ values were determined from the intersection of two tangential lines in the plot. However, the structural relaxation made it difficult to find out $T_g$ which is a point of a rapid change on the plot, so the $T_g$ could not be determined in this plot. Therefore, the calculation of the viscous flow was conducted to identify value of $T_g$ using the TMA experiment.

Figure 4(a) and (b) show the typical viscosity measurement using the Stefan equation (see Eq. (1)):

$$\eta = -\frac{2Fh^3}{3\pi a^4\left(\frac{dh}{dt}\right)} \quad (1)$$

where $F$ is the applied load, a is the radius of the plates, and h is the height of the sample [26]. In the supercooled liquid region ($\Delta T_x = T_{x,TMA} - T_g$), the viscosity is decreased; therefore, the $T_g$ was determined the onset point of the rapid decrease of viscosity. In general, $T_{x,TMA}$ is considered as the temperature with the lowest viscosity ($T_{vs}$) in the viscosity curves, because the viscosity decreased with an increase of the temperature until the onset of crystallization [27-29]. The values of $T_g$, $T_{x,TMA}$, and $T_{vs}$ are marked with the arrows in Fig. 4(b). However, $T_{vs}$ of alloys with x = 0, 1, 2 almost corresponds to $T_{x,DSC}$ and

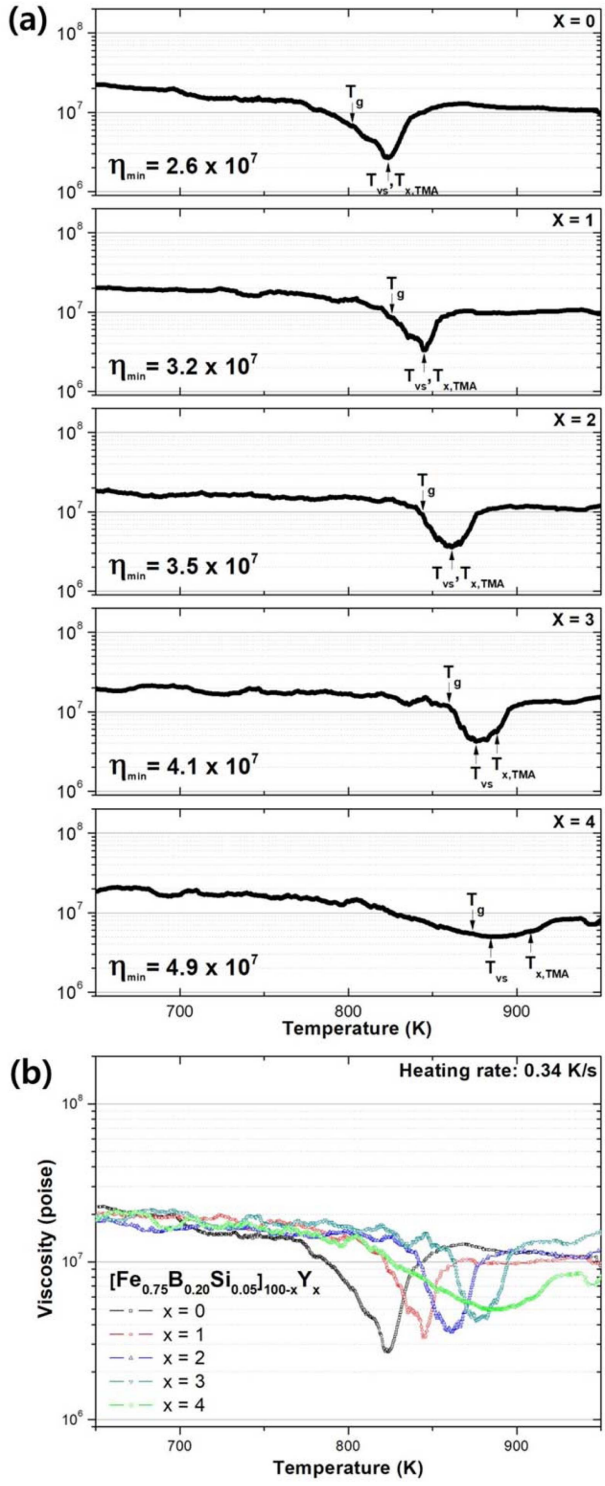


**Fig. 4.** (Color online) (a) Temperature dependence of the effective viscosity for the $[Fe_{0.75}B_{0.20}Si_{0.05}]_{100-x}Y_x$ (x = 0, 1, 2, 3, 4) melt-spun ribbons and (b) the viscosity curves are separated for clarity.

$T_{x,TMA}$, while the alloys with x = 3 and x = 4 do not correspond to those values. The measured viscosity

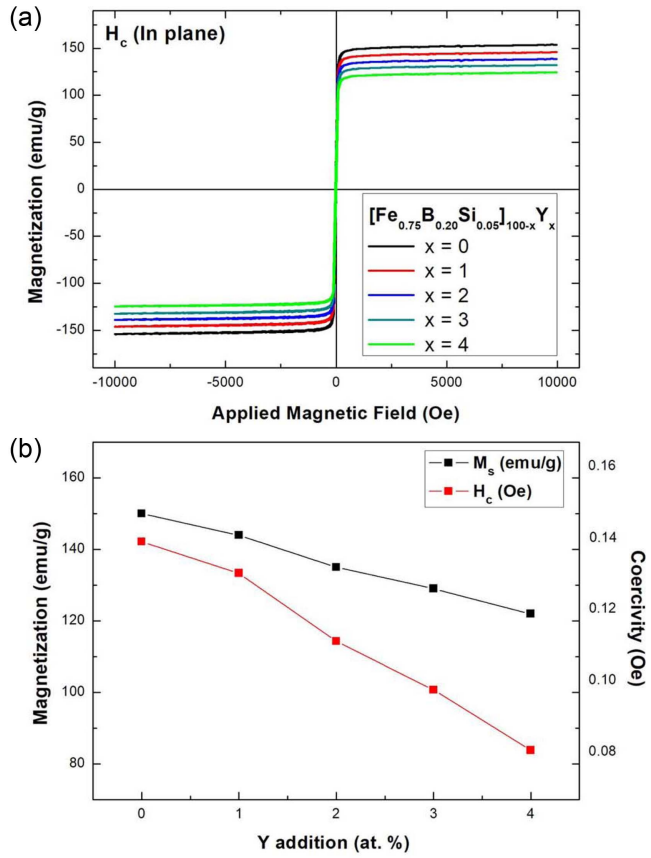


**Fig. 5.** (Color online) (a) Hysteresis loops and (b) variation of $M_s$ and $H_c$ with an increase of the Y content.

increased in the range from $2.6 \times 10^7$ to $4.9 \times 10^7$ poise, suggesting that atomic diffusion more difficult. As a result, the kinetics behavior slowed down; therefore, it would take longer time to reach the metastable equilibrium state. In summary, $T_{vs}$ of $Fe_{72.75}B_{19.4}Si_{4.85}Y_3$ (x = 3) and $Fe_{72}B_{19.2}Si_{4.8}Y_4$ (x = 4) alloys did not correspond to $T_{x,DSC}$ and $T_{x,TMA}$ due to slow kinetic behavior in the crystallization region. Therefore, $T_{x,TMA}$ was not determined as the $T_{vs}$ in the viscosity curves. The thermal properties are summarized in Table 1. As can be seen in Table 1, $T_{x,TMA}$ values almost correspond to $T_{x,DSC}$. The values of $\Delta T_x$ increased from 18 to 41 K with an increase of the Y content, which suggests that the addition of the Y content improved the GFA of $[Fe_{0.75}B_{0.20}Si_{0.05}]_{100-x}Y_x$ (x = 0, 1, 2, 3, 4). It was caused by the oxygen scavenging effect through the formation of yttrium oxide during arc-melting and melt-spinning processes [30, 31].

**Table 2.** Magnetic properties of the $[Fe_{0.75}B_{0.20}Si_{0.05}]_{100-x}Y_x$ (x = 0, 1, 2, 3, 4) melt-spun amorphous ribbons.

| | | | | | Magnetic Properties | |
|---|---|---|---|---|---|---|
| x | Alloys | | | | $H_c$ (Oe) | $M_s$ (emu/g) |
| 0 | $Fe_{75}$ | $B_{20}$ | $Si_5$ | | 0.14 | 150.0 |
| 1 | $Fe_{74.25}$ | $B_{19.8}$ | $Si_{4.95}$ | $Y_1$ | 0.13 | 144.3 |
| 2 | $Fe_{73.5}$ | $B_{19.6}$ | $Si_{4.9}$ | $Y_2$ | 0.11 | 135.3 |
| 3 | $Fe_{72.75}$ | $B_{19.4}$ | $Si_{4.85}$ | $Y_3$ | 0.10 | 129.6 |
| 4 | $Fe_{72}$ | $B_{19.2}$ | $Si_{4.8}$ | $Y_4$ | 0.08 | 122.8 |

The magnetization curves of the $[Fe_{0.75}B_{0.20}Si_{0.05}]_{100-x}Y_x$ (x = 0, 1, 2, 3, 4) amorphous ribbons are shown in Fig. 5(a). All specimens exhibited soft magnetic properties with a high $M_s$ of 150-122.8 emu/g and low $H_c$ of 0.14-0.08 Oe. With an increase of the Y content, the values of $M_s$ decreased due to the reduction of the content of Fe [29, 32]. The values of $H_c$ decreased an increase of the Y content as well. Fig. 5(b) shows the variations of $M_s$ and $H_c$ with an increase of the Y content, and the magnetic properties are reported in Table 2.

## 4. Conclusion

In this study, we investigated whether a small amount of Y addition would have a significant effect on the thermal and soft magnetic properties for $[Fe_{0.75}B_{0.20}Si_{0.05}]_{100-x}Y_x$ (x = 0, 1, 2, 3, 4) amorphous alloy systems. All ribbons were identified as fully amorphous in the XRD patterns. The DSC and TMA curves provide the GFA and viscous flow. The widest $\Delta T_x$ was obtained at the highest Y content of 4 at.%. Therefore, it can be concluded that the improvement of GFA was brought by the addition of Y with the larger radius difference with Fe. In addition, the measured viscosity increased with an increase of the Y content, this results support the statement that the atomic diffusion is more difficult due to an increase of the Y content. In terms of magnetic properties, through the M-H curves, it is confirmed that the values of $M_s$ and $H_c$ decreased with an increase of the Y content.

In conclusion, we studied with varying Y content to investigate the Y effects based on the empirical rules. As a result, it is noted that the addition of Y is effective in improvement of GFA and reduction of $H_c$. Therefore, in the future, a good combination of high GFA for the present alloys can lead to the production of a new soft-magnetic material characterized by high thermal stability.

## Acknowledgements

This research was supported by Basic Science Research Program through the National Research Foundation of Korea (NRF) funded by the Ministry of Science, ICT & Future Planning (MSIP) (2018006784).

## References


[1] C. Suryanarayana and A. Inoue, Int. Mater. Rev. **58**, 131 (2013).
[2] D. C. Jiles, Acta Mater. **51**, 5907 (2003).
[3] T. D. Shen and R. B. Schwarz, Appl. Phys. Lett. **75**, 49 (1999).
[4] M. Pasquale, J. Magn. **8**, 60 (2003).
[5] P. Duwez and S. C. H. Lin, J. Appl. Phys. **38**, 4096 (1967).
[6] A. Inoue, Y. Shinohara, and J. S. Gook, Mater. Trans. JIM **36**, 1427 (1995).
[7] B. Shen, M. Akiba, and A. Inoue, Appl. Phys. Lett. **88**, 131907 (2006).
[8] R. C. O'handley, J. Appl. Phys. **62**, R15 (1987).
[9] G. Herzer, Acta Mater. **61**, 718 (2013).
[10] H. S. Chen, Rep. Prog. Phys. **43**, 353 (1980).
[11] M. Chen, NPG Asia Mater. **3**, 82 (2007).
[12] W. H. Wang, Prog. Mater Sci. **52**, 540 (2007).
[13] F. L. Kong, C. T. Chang, A. Inoue, E. Shalaan, and F. Al-Marzouki, J. Alloy. Compd. **615**, 163 (2014).
[14] S. M. Kim, B. K. Han, and H. Choi-Yim, J. Magn. **21**, 164 (2016).
[15] Y. B. Kim, D. H. Jang, H. K. Seok, and K. Y. Kim, Mater. Sci. Eng. A **449-451**, 389 (2007).
[16] Z. B. Jiao, H. X. Li, J. E. Gao, Y. Wu, and Z. P. Lu, Intermetallics **19**, 1502 (2011).
[17] B. K. Han, H. J. Jo, J. K. Lee, K. B. Kim, and H. Yim, J. Magn. **18**, 395 (2013).
[18] A. Inoue, Mater. Trans. JIM **36**, 866 (1995).
[19] J. H. Kim, J. S. Park, E. Fleury, W. T. Kim, and D. H. Kim, Mater. Trans. **45**, 2770 (2004).
[20] T. Bitoh and D. Watanabe, Metals **5**, 1127 (2015).
[21] F. R. De Boer, R. Boom, W. C. M. Matterns, A. R. Miedema, and A. K. Niessen, Cohesion in Metals, North-Holland, Amsterdam (1989) p 217.
[22] T. Nakamura, E. Matsubara, M. Imafuka, H. Koshiba, A. Inoue, and Y. Waseda, Mater. Trans. **42**, 1530 (2001).
[23] J. Zhang, C. Chang, A. Wang, and B. Shen, J. Non-Cryst. Solid **358**, 1443 (2012).
[24] T. Yamasaki, S. Maeda, Y. Yokoyama, D. Okai, T. Fukami, H. M. Kimura, and A. Inoue, Intermetallics **14**, 1102 (2006).
[25] M. Q. Jiang, M. Naderi, Y. J. Wang, M. Peterlechner, X. F. Liu, F. Zeng, F. Jiang, L. H. Dai, and G. Wilde, AIP Adv. **5**, 127133 (2015).
[26] G. J. Dienes and H. F. Klemm, J. Appl. Phys. **17**, 458 (1946).
[27] E. Bakke, R. Busch, and W. L. Johnson, Appl. Phys. Lett. **67**, 3260 (1995).
[28] R. Busch, E. Bakke, and W. L. Johnson, Acta. Mater. **46**, 4725 (1998).
[29] J. Oh, J. Y. Suh, W. J. Kim, J. I. Jang, K. H. Kang, C. S. Yoon, and H. Choi-Yim, Curr. Appl. Phys. **18**, 411 (2018).
[30] Z. P. Lu, C. T. Liu, and W. D. Porter, Appl. Phys. Lett. **83**, 2581 (2003).
[31] J. M. Park, J. S. Park, J. H. Na, D. H. Kim, and D. H. Kim, Mater. Sci. Eng. A **435-436**, 425 (2006).
[32] Z. Long, Y. Shao, F. Xu, H. Wei, Z. Zhang, P. Zhang, and X. Su, Mater. Sci. Eng. B **164**, 1 (2009).